Aluminium fumarate and CPO-27(Ni) MOFs

Hussein, Eman; Al-Dadah, Raya; Mahmoud, Saad; Elsayed Ali Hussin, Ahmed; Anderson, Paul

DOI:
10.1016/j.applthermaleng.2016.01.129

Accepted Manuscript

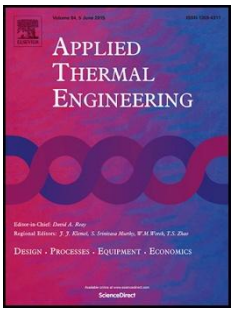

Title: Aluminium fumarate and CPO-27(Ni) MOFs: Characterization and Thermodynamic Analysis for Adsorption Heat Pump Applications.

Author: Eman Elsayed, Raya AL-Dadah, Saad Mahmoud, Ahmed Elsayed, Paul A. Anderson

PII: S1359-4311(16)30079-5
DOI: http://dx.doi.org/doi: 10.1016/j.applthermaleng.2016.01.129
Reference: ATE 7689

To appear in: *Applied Thermal Engineering*

Received date: 13-8-2015
Accepted date: 26-1-2016

Please cite this article as: Eman Elsayed, Raya AL-Dadah, Saad Mahmoud, Ahmed Elsayed, Paul A. Anderson, Aluminium fumarate and CPO-27(Ni) MOFs: Characterization and Thermodynamic Analysis for Adsorption Heat Pump Applications., *Applied Thermal Engineering* (2016), http://dx.doi.org/doi: 10.1016/j.applthermaleng.2016.01.129.

Aluminium fumarate and CPO-27(Ni) MOFs: Characterization and Thermodynamic Analysis for Adsorption Heat Pump Applications.

Eman Elsayed[a,b,*], Raya AL-Dadah[a], Saad Mahmoud[a], Ahmed Elsayed[a], Paul A. Anderson[b]

[a] School of Mechanical Engineering, University of Birmingham, Birmingham, B15 2TT, United Kingdom.

[b] School of Chemistry, University of Birmingham, Birmingham, B15 2TT, United Kingdom.

* Corresponding author. E-mail: EXH496@student.bham.ac.uk ; Tel.: 07477373797.

Highlights:

- CPO-27(Ni) and aluminium fumarate were investigated for adsorption heating, cooling and desalination applications.
- Both MOFs have high potential in adsorption applications.
- The optimum desorption temperature, for the CPO-27(Ni) is higher than 90^{o}C and for aluminium fumarate is 55-70^{o}C.
- CPO-27(Ni) outperforms aluminium fumarate at low evaporation temperature (5^{o}C).
- Aluminium fumarate outperforms CPO-27(Ni) at high evaporation temperature (20^{o}C).

Abstract

Metal-Organic Framework (MOF) materials are new porous materials with high surface area, pore size and volume, and tunable pore geometry thus providing high adsorption capacity. Currently, limited MOF materials with high water adsorption capabilities and hydrothermal stability are available on a large scale. Two MOF materials namely CPO-27(Ni) and aluminium fumarate have been identified to have a high hydrothermal stability, high water uptake of 0.47 $g_{H2O}.g_{ads}^{-1}$ and 0.53 $g_{H2O}.g_{ads}^{-1}$ at a relative pressure of 0.9 and are commercially available.

This work aims to measure the water adsorption characteristics of these two MOF materials in terms of isotherms, kinetics and cyclic stability. Also the thermodynamic cycle performance of such materials based on their equilibrium adsorption data was investigated under different operating conditions for various adsorption applications such as heating, cooling and water desalination.

Results showed that the CPO-27(Ni)/water pair outperformed the aluminium fumarate/water pair at low evaporation temperatures (5^{o}C) and high desorption temperatures (≥ 90^{o}C), while the aluminium fumarate/water pair was more suitable for applications requiring high evaporation temperature (20^{o}C) and/or low desorption temperature (70^{o}C).

Keywords: Metal-Organic Framework**,** Characterization, Adsorption, Heat pump, Refrigeration, Desalination.

Nomenclature

	Description	*Unit*
A	Adsorption potential	$J.mol^{-1}$
COP	Coefficient of performance	--
D_{so}	Pre-exponential constant of the effective vapour diffusivity	$m^2.s^{-1}$
D_s	Surface diffusion coefficient	$m^2.s^{-1}$
E	Adsorption characteristic parameter	$J.mol^{-1}$
E_a	Activation energy	$J.mol^{-1}$
F	Constant depending on the particles shape	--
ΔH_{ads}	Isosteric heat of Adsorption	$J.kg^{-1}$
$K_s a_v$	Overall mass transfer coefficient	S-1
k_0	LDF model empirical constant	s^{-1}
n	Exponent fitting parameter	--
OPR	Overall Performance Ratio	--
P	Equilibrium pressure	Pa
P_C	Condenser pressure	Pa
P_E	Evaporator pressure	Pa
P_s	Saturation pressure of adsorbate at adsorption temperature	Pa
P/P_s	Relative pressure	--
Q_{ads}	Heat of adsorption	kJ
Q_c	Heat of condensation	kJ
Q_{des}	Heat of desorption	kJ
Q_e	Heat of evaporation	kJ
R	Ideal gas constant	$J.(mol.K)^{-1}$
R_p	Radius of adsorbent particle	m
T	Temperature	K
T_{Ads}	Adsorber temperature	^oC
T_C	Condenser temperature	^oC
T_{Des}	Desorption temperature	^oC
T_E	Evaporator temperature	^oC
X	Equilibrium uptake	$g_{H2O}.g_{ads}^{-1}$
x_0	Maximum uptake	$g_{H2O}.g_{ads}^{-1}$

1. Introduction

Metal-Organic Frameworks (MOF) are highly crystalline materials, with high surface area and pore volume, that are moderately stable and can be synthesized in a very pure form and thus have great potential for various applications like catalysis [1], gas separations and storage [2], sensors [3] and heat pumps [4]. The adsorption performance of a number of MOFs including ISE-1, HKUST-1, MIL-100(Fe), MIL-53(Fe), Basolite 100A and Basolite F300 were investigated, showing high adsorption capabilities compared to silica gel and zeolite [5-12]. Also, the heat of adsorption for MOFs was found to be lower than the heat of adsorption for zeolites, which means a lower interaction between the framework and the water molecules and a lower regeneration temperature is required. HKUST-1 unlike most of the MOFs showed a significant degradation in its cycle stability due to the destruction of the structure, limiting its use in water adsorption applications. Another significant advantage of MOFs, is that the water vapour capacity can vary as the organic linker and the metal cluster changes resulting in tunable properties leading to a better performance. This advantage is very apparent in MIL-101(Cr) which has a high water uptake of 1-1.43 $g_{H2O}.g_{ads}^{-1}$(at high relative pressure > 0.35) and a high cyclic stability [13-18]. The crucial problem with most MOFs is the commercial availability which limits use in many applications.

CPO-27(Ni) (known as MOF-74(Ni)) and aluminium fumarate are two MOFs that have high water adsorption capabilities of $0.47 g_{H2O}.g_{ads}^{-1}$ and $0.53\ g_{H2O}.g_{ads}^{-1}$, respectively. The two materials are hydrothermally stable [19-20] and due to the previous properties they have the potential to be used in adsorption heat pump applications. The most important advantage of these two MOFs is that they are synthesized and commercially produced by Johnson Matthey and MOFs technologies respectively.

The main objective of this work is to assess the water adsorption characteristics of these MOFs and investigate their performance under various operating conditions for different adsorption applications such as heating, cooling and water desalination.

2. Experimental Work:

This section describes techniques used to characterize the two MOFs through particle size, powder X-Ray Diffraction (XRD), N_2 adsorption and water adsorption characteristics using a Dynamic Vapour Adsorption analyser (DVS). The equilibrium water adsorption characteristics were then used to develop the P-T-x diagrams required to assess the two MOFs suitability for the various adsorption applications.

The particle size of the two materials was measured using a Delsa™Nano Particle Size analyser.

The powder XRD patterns were measured using a Bruker D8 Advance Reflection Diffractometer with Cu Kα radiation (1.5418 Å). The aluminium fumarate sample was scanned from 8 to 45° 2θ and the CPO-27(Ni) sample from 10 to 75°, with a step size of 0.02° and both samples were spun at 15 rpm.

The N_2 adsorption isotherm at 77 K was used to measure the BET surface area [21] using a Quantachrome NOVA surface area analyser.

The dynamic vapour sorption (DVS) gravimetric analyser (Advantage DVS, Surface Measurement Systems, UK) (**Fig. S1**) was used to study the water adsorption characteristics [7, 22]. The water adsorption isotherms were measured at 15°C, 25°C and 35°C for aluminium fumarate and at 25°C, 35°C and 55°C for CPO-27(Ni).
(See supporting information, S1)

3. Theory:

3.1. Adsorption Isotherm models:

The measured adsorption isotherms for water vapour onto CPO-27(Ni) at 25°C, 35°C and 55°C were fitted using the Dubinin-Astakhov equation (**Eq. 1**) commonly used for adsorption equilibrium of gases and vapours onto microporous adsorbents [25]:

$$X = x_0 Exp\ (-(\frac{A}{E})^n) \quad \textbf{(1)}$$

$$A = RT\ \ln(\frac{P}{P_s}) \quad \textbf{(2)}$$

In the case of aluminium fumarate, to predict the water uptake at wide range of operating temperatures and pressure, the measured adsorption isotherms at 15°C, 25°C and 35°C were fitted using a series of equations (exponential and polynomial) in terms of X and A.

3.2. Adsorption kinetic models:

The rate of adsorption or the adsorption kinetics is another crucial parameter determining the residence time required for completion of the adsorption cycle and depending on the interaction between the adsorbent and the adsorbate.
The Linear Driving Force model [26, 27, 28] (**Eq. 3-6**) has been one of the most used kinetics model as it is applicable to a wide range of adsorbents [29, 30, 31]

$$\frac{dx}{dt} = K_s a_v \cdot (X - x_0) \quad \textbf{(3)}$$

$$\frac{dx}{dt} = k_0 \cdot Exp\left[-\frac{E_a}{RT}\right] \cdot (X - x_0) \quad \textbf{(4)}$$

$$k_0 = \frac{F.D_{so}}{R_p^2} \quad \textbf{(5)}$$

$$D_s = D_{so}.Exp\left[-\frac{E_a}{RT}\right] \quad \textbf{(6)}$$

Where F is a constant depending on the shape of the adsorbent particles which is 15 for spherical particles and 8 for cylindrical particles.

The values of the different isotherms and kinetic equations parameters are calculated and discussed in section 4.

3.3. MOF-based adsorption cycle:

In the adsorption cycle, a working fluid is evaporated, taking its evaporation heat Q_{evap} from the surroundings and thereby producing useful cold in cooling applications. Then vapour is adsorbed into the porous material, generating adsorption heat Q_{ads}, which is larger than the latent heat of vaporization (usually by 10-30%) [19, 20, 25]. This heat is released to the environment in the cooling case or produces useful heat in the heat pump application. In the desorption process, the porous material is regenerated by applying heat Q_{des} from various external heat sources like solar energy or industrial waste heat. The desorbed fluid condenses at a medium temperature level, releasing the heat of condensation Q_{cond}. This is useful in the heat pump and is released to the environment in cooling applications [16]. Equilibrium adsorption characteristics of a gas or vapour on a solid can be depicted in the P-T-x diagrams.

The specific heat of adsorption can be calculated through the Clausius–Clapeyron equation (**Eq. 7**):

$$\Delta H_{ads} = -R_{water} \frac{\partial \ln(P)}{\partial (\frac{1}{T})} \quad \textbf{(7)}$$

The cooling effect in the cycle occurs during the isobaric adsorption process when the adsorbate is evaporated by gaining heat from the surroundings. The heating effect appears during the isobaric desorption process when the adsorbate is condensed by releasing heat to surroundings. The Coefficient of Performance (COP) is measured by the ratio of the useful energy provided by the device to the required input [19, 23, 32, 33]. For applications such as heat pumps, where the useful energy is the heat supplied by the condenser and the adsorption bed, COP_h can be defined as:

$$COP_h = \frac{Q_{ads} + Q_c}{Q_{des}} \quad \textbf{(8)}$$

For cooling applications like water chillers, the useful energy from the device is the evaporation energy, and hence:

$$COP_{ref} = \frac{Q_e}{Q_{des}} \quad \textbf{(9)}$$

Adsorption Desalination, is a novel adsorption system producing two useful effects, namely high grade potable water and cooling with only a single heat source input (low grade heat source of temperatures from 50°C to 85°C) [34, 35].The performance of the system can be expressed through COP_{ref} or the Overall Performance Ratio (OPR) [35]:

$$OPR = \frac{Q_e + Q_c}{Q_{des}} \quad \textbf{(10)}$$

4. Results and discussion

4.1. Powder X-Ray Diffraction:

Fig. S2 shows the powder XRD patterns of both MOFs. The sharp peaks of the CPO-27(Ni) pattern highlight the high crystallinity of the material, while the very broad peaks of aluminium fumarate are consistent with the small crystallite size (grain size) measurement. The average particle size of the aluminium fumarate was 1.3 µm and the CPO-27(Ni) was 107.5 µm.

4.2. Surface area measurements:

Fig. S3 shows the N_2 adsorption isotherm at 77 K for both MOF materials. It is clear that aluminium fumarate had a higher N_2 adsorption capacity than that of CPO-27(Ni) and hence a higher surface area, giving a BET surface areas of 893.965 $m^2.g^{-1}$ and 469.777 $m^2.g^{-1}$, respectively.

4.3. Water adsorption isotherms:

Fig. 1 shows the measured water adsorption/desorption isotherms at a temperature of 25°C for both MOFs.

From the figure, CPO-27(Ni) exhibited a type I adsorption isotherm with no hysteresis reaching 81% of its capacity at a very low relative pressure and then a plateau reaching its maximum uptake of 0.47 $g_{H2O}.g_{ads}^{-1}$ at a relative pressure of 0.9. This performance is due to the presence of unsaturated metal centres (UMCs) existing in some MOF structures. These UMCs are metal binding sites formed after the removal of axial ligands from metal atoms attracting water molecules and offering extra binding sites to the guest molecules, especially at low pressure values [23]. On the other hand, the strong interaction between the water molecules and these sites requires a higher desorption temperature. To further investigate the performance of the material at different temperatures, the water adsorption isotherm of the material was also measured at 35°C and 55°C (**Fig. S4**).The material showed almost the same uptake over the investigated temperature range.

On the other hand, aluminium fumarate exhibited a type IV isotherm with type H1 hysteresis indicating a narrow distribution of uniform pores. **Fig. 1** shows that at low partial pressure (below 0.2), the water uptake was low, but a steep increase in the water uptake took place at a relative pressure range between 0.2 and 0.3 to reach 0.35 $g_{H2O}.g_{ads}^{-1}$ and then the uptake continued to increase till it reached the maximum value of 0.53 $g_{H2O}.g_{ads}^{-1}$ at a relative pressure of 0.9.

The adsorption mechanism of aluminium fumarate differs from that of the CPO-27(Ni). In aluminium fumarate, the water molecules are uniformly accumulated in the inner pores of the material indicating the hydrophilicity of the inner pore surface, without the presence of unsaturated metal sites.

The limited water uptake at low relative pressure in aluminium fumarate is related to the hydrophobicity of the organic linker [24]. The water adsorption isotherm of the material was also measured at 15°C and 35°C (**Fig. S5**) to investigate the performance of the material at different temperatures and the material showed almost the same uptake over the investigated temperature range.

In order to evaluate performance stability, the two materials were exposed to ten successive water adsorption/desorption cycles. CPO-27(Ni) showed great performance stability with a negligible decrease of only 0.35% (**Fig. 2a**). Aluminium fumarate showed a higher decrease during the first 4 cycles (**Fig. 2b**) and a stable performance afterwards which could be attributed to the breathing phenomenon observed in some MOFs like MIL-53 causing the thermodynamic water sorption equilibrium to not be completely reached within the first cycles. The material was reported to exhibit a stable performance after the first few cycles [20].

4.4. Adsorption isotherm models:

The equilibrium adsorption isotherm data was fitted through Dubinin-Astakhov equation (**Eq. 1**). **Table 1** gives the values of parameters x_0, E and n.

The equilibrium water adsorption data was fitted through (Eq. **11-13)** to predict the water uptake of aluminium fumarate at different adsorption temperatures:

$$X = 0.111993 \quad Exp\ (-0.000258797 \quad A) \qquad \textbf{A>3987} \qquad \textbf{(11)}$$

$$X = 2.36129 \quad -9.93768 \quad E-04\ A + 1.05709 \quad E-07\ A^2 \qquad \textbf{2900} \leq \textbf{A} \leq \textbf{3987} \qquad \textbf{(12)}$$

$$X = -3.124455 \quad E-11\ A^3 + 1.68302 \quad E-07\ A^2 - 3.12\ E-04\ A + 0.5948 \qquad \textbf{A<2900} \qquad \textbf{(13)}$$

Fig. **S6 & S7**, highlight the validity of the Dubinin-Astakhov model and the proposed equations to fit the experimental data for both materials at different adsorption temperature.

4.5. Adsorption kinetics models:

The rate of water adsorption was simulated through applying the LDF model. **Table 2** gives the values of parameters E_a and k_0, R_p and D_{so} .**Table 3** indicate the effect of temperature on the diffusion coefficient, as increasing the temperature will increase the surface diffusion coefficient.

Fig. S8, highlights the validity of the LDF model to fit the experimental data for both materials. The values of LDF equation parameters are shown in (**Tables 2 & 3**) where it is evident that the diffusion coefficient of aluminium fumarate is lower than that of CPO-27(Ni)**.** This is in agreement with **Fig. 3** showing the time variation of the measured fractional uptake of the two adsorbents, it is clear that the CPO-27(Ni) reached equilibrium much faster than aluminium fumarate. Also, **Fig. S9** presents the measured water vapour uptake variation with time for CPO-27(Ni) and aluminium fumarate using different vapour pressures at 25°C. The figures indicate the difference in the adsorption rate between

the two MOFs showing that the kinetics in case of aluminium fumarate is significantly more passive than in CPO-27(Ni).

The slower kinetics of aluminium fumarate may be attributed to the absence of the UMCs and the domination of the hydrophobicity of the organic ligand at low pressures. The faster adsorption rate of CPO-27(Ni)/water pair implies the potential of utilizing CPO-27(Ni) in applications requiring short adsorption/desorption cycle time.

Based on the previously discussed equilibrium water adsorption data, the effect of different operating conditions on the performance of aluminium fumarate/water and CPO-27(Ni)/water were investigated to assess their suitability for various applications. The performance of the two materials was assessed through assuming ideal thermodynamic cycles. Thermodynamic relationships between pressure, adsorption temperature and water vapour concentration, as depicted in the P-T-x diagram (**Fig. 4**), were used to calculate the COP and water vapour concentration difference of each cycle. Condensation temperatures from 30^{o}C to 45^{o}C were investigated. The adsorption temperature was assumed to be equal to the condensation temperature. The effect of increasing the regeneration temperature from 70^{o}C to 110^{o}C was also investigated, and finally the effect of evaporation temperature on the thermodynamic cycle of the two materials was discussed with evaporation temperatures of 5^{o}C and 20^{o}C.

4.6. Effect of regeneration and condensation temperature on the performance of aluminium fumarate/water and CPO-27(Ni)/water pairs at an evaporation temperature of 5^{o}C:

Fig. 5 illustrates the effect of condensation and regeneration temperatures on the COP_h and COP_{ref} of CPO-27(Ni) and aluminium fumarate cycles using an evaporation temperature of 5^{o}C. It can be seen that as the regeneration temperature increases, the COP_h and COP_{ref} increase to reach a maximum and then remains relatively constant within the tested temperature range. However, the effect of the regeneration temperature is higher in the case of CPO-27(Ni) than in the case of aluminium fumarate. For example, for CPO-27(Ni), increasing the regeneration temperature from 70^{o}C to 110^{o}C at a constant condensation temperature of 30^{o}C increases the COP_h from 1.35 to 1.67. This can be explained by the difference in water loading for the two materials at various regeneration temperatures (**Fig. 6**) where increasing the regeneration temperature from 70^{o}C and 110^{o}C, increases the water loading difference from 0.034 to 0.355 l/kg for CPO-27(Ni) and from 0.014 to 0.023 l/kg for aluminium fumarate.

However, in case of the aluminium fumarate at a condensation temperature of 30^{o}C, the COP_h increased with increasing the regeneration (desorption) temperature to reach a maximum value of 1.408 at 85^{o}C and then decreased with further increase in the regeneration temperature to reach 1.388 at 110^{o}C. A similar behaviour was observed in some carbon materials [36, 37]. This behaviour is due to the fact that aluminium fumarate material is almost dry at a relative pressure of 0.2 (**Fig. 1**) corresponding to a desorption temperature of ~55^{o}C at a condensation temperature

of 25°C (65°C [20]). Thus increasing the regeneration temperature will not desorb more water vapour but will contribute to increasing heat losses in the cycles.

Also the figure shows that increasing the condensation temperature from 30°C to 45°C adversely affects the COP_h. This behaviour can be attributed to the increase in the water vapour concentration at the end of the cycle, decreasing the water circulated and eventually decreasing the efficiency of the cycle.

Finally, it is observable from **Fig. 5** that the effect of condensation and regeneration temperature on the COP_{ref} follows the same trend as the COP_h and it can be concluded that CPO-27(Ni) outperforms aluminium fumarate at low evaporation temperatures (5°C).

For other adsorption applications like adsorption desalination, the amount of distilled water produced is an essential parameter in choosing the adsorbent type and the operating conditions. **Fig. 6** illustrates the effect of condensation and regeneration temperatures on the amount of distilled water that can be produced as 'water loading difference' from CPO-27(Ni) and aluminium fumarate cycles using an evaporation temperature of 5°C. From the figure, increasing the condensation temperature decreases the water loading difference for both MOFs, while increasing the regeneration temperature from 70°C to 110°C increases it profoundly in CPO-27(Ni) but only slightly in case of aluminium fumarate. This illustrates the considerable dependence of CPO-27(Ni) performance on the regeneration temperature. This dependence can be related to the isosteric heat of adsorption, for CPO-27(Ni) it was found to be higher (16 % higher than the specific heat of vaporization of water) than that of aluminium fumarate (10 % higher than the specific heat of vaporization of water).

The figure also highlights the potential of using CPO-27(Ni) in adsorption desalination cycles operated at low evaporation and high regeneration temperatures producing a dual effect of water production as high as 0.35 l/kg per cycle and a COP_{ref} of 0.67.

Based on **Fig. 6**, it is doubtless that at an evaporation temperature of 5°C, only the CPO-27(Ni) can be used in an adsorption desalination system but the system should be operated at a high regeneration temperature (≥90°C). To further assess the system the Overall Performance Ratio (OPR) was estimated.

Fig.7 shows the effect of regeneration and condensation temperatures on the OPR of the desalination system. It is evident that increasing the condensation temperature would negatively affect the OPR of the system, while increasing the regeneration temperature would improve its performance.

4.7. Effect of regeneration and condensation temperature on the performance of aluminium fumarate/water and CPO-27(Ni)/water pairs at an evaporation temperature of 20°C:

Fig. 8 illustrates the effect of condensation and regeneration temperature on the COP_h of CPO-27(Ni) and aluminium fumarate cycles using an evaporation temperature of 20°C. It is noticeable that increasing the condensation temperature would decrease the COP_h of CPO-27(Ni) cycle while it

would only affect the performance of the aluminium fumarate at a condensation temperature higher than 40°C. Increasing the regeneration temperature from 70°C to 110°C would increase the COP_h of CPO-27(Ni) and decrease the COP_h of aluminium fumarate.

When comparing the effect of the evaporation temperature, **Fig. 5** and **Fig. 8**, it can be noticed that increasing the evaporation temperature will improve the performance of aluminium fumarate very significantly but less notably in the case of CPO-27(Ni).In other words, porous materials with a type I adsorption isotherm would not be significantly affected by increasing the evaporation temperature as much as materials possessing a type IV isotherm.

It is also evident that the effect of increasing the condensation and regeneration temperature on the COP_{ref} follows the same behaviour as on the COP_h.

Fig. 9 illustrates the effect of condensation and regeneration temperature on the amount of water produced (water loading difference) from the CPO-27(Ni) and aluminium fumarate cycles using an evaporation temperature of 20°C. It is evident that in the case of both MOFs, increasing the condensation temperature would adversely affect the water loading difference. Also, increasing the regeneration temperature would increase the distilled water produced from both MOFs.

Comparing **Fig. 6** and **Fig. 9**, it is shown that increasing the evaporation temperature from 5°C to 20°C would significantly increase the distilled water produced from the aluminium fumarate cycle as the water loading difference increased to 0.47 l/kg at an evaporation temperature of 20°C. This can be attributed to the fact that the material exhibits a type IV isotherm where its uptake increases significantly with increasing the evaporation temperature. Increasing the evaporation temperature was found to have a limited effect on the amount of water produced from CPO-27(Ni) as the material exhibits a type I water adsorption isotherm reaching 81% of its capacity at a very low relative pressure and hence less dependent on the evaporation temperature.

Based on the amount of the distilled water that can be produced from the CPO-27(Ni) and aluminium fumarate at an evaporation temperature of 20°C, the CPO-27(Ni) can only be used at a high regeneration temperature ($\geq$ 90°C), while aluminium fumarate can be used at a regeneration temperature as low as 70°C. To further assess the potential for desalination systems, the OPR was estimated.

Fig. 10 shows the effect of regeneration and condensation temperature on the OPR of the desalination cycles. It is evident that increasing the condensation temperature would profoundly decrease the OPR of the CPO-27(Ni) cycle, while it would have a slight effect on aluminium fumarate cycle. Increasing the regeneration temperature would enhance the performance of the CPO-27(Ni) desalination system, while it would negatively affect the OPR of the aluminium fumarate cycle based on COP_h, COP_{ref} and water loading difference figures.

Fig. 5-10 highlight that the aluminium fumarate is found to outperform CPO-27(Ni) at high evaporation temperature (20°C) while it is the opposite at low evaporation temperature (5°C).Also, Based on the adsorption kinetics, CPO-27(Ni) is more suitable for heat-powered adsorption heating and cooling applications where high temperature heat sources are available and short adsorption/desorption cycle time is required. On the contrary, the aluminium fumarate seems to be more suitable for solar adsorption applications where lower regeneration temperatures are used and comparatively longer cycle time is required.

The potential adsorption applications of aluminium fumarate and CPO-27(Ni) and the suitable operating conditions based on the investigated temperature ranges are summarized in **Table 4**.

5. Conclusion:

Metal-Organic Framework materials offer great potential for a wide range of thermally driven adsorption applications like cooling, heating and water desalination. This paper characterizes two commercially available MOFs namely aluminium fumarate and CPO-27(Ni) (MOF-74(Ni)) and investigates their performance for various adsorption applications.

Results showed that increasing the regeneration temperature would adversely affect the COP of aluminium fumarate while it improve it in case of CPO-27(Ni) in the investigated temperature range. On the other hand, increasing the condensation temperature was found to be detrimental to the performance of the two materials.

The CPO-27(Ni) was found to be more suitable for applications working at a low evaporation temperature (5°C) and high regeneration temperature (≥90°C) achieving a COP_{ref} higher than 0.6, while aluminium fumarate showed a superior performance at a higher evaporation temperature (20°C) and low regeneration temperature (70°C). Both materials showed a great potential for the adsorption desalination application.

This work paves the way for using aluminium fumarate and CPO-27(Ni) in thermally driven adsorption systems, highlighting their potential in adsorption desalination and also in adsorption heat pump applications that are currently dominated by conventional porous materials such as silica gel and zeolites.

References:

[1] Yoon M, Srirambalaji R, Kim K, Homochiral Metal–Organic Frameworks for Asymmetric Heterogeneous, Catalysis, Chem. Rev 2012;112:1196-1231.

[2] Suh M, Park H, Prasad T, Lim D, Hydrogen Storage in Metal–Organic Frameworks, Chem. Rev 2012;112:782-835.

[3] Kreno L, Leong K, Farha O, Allendorf M, van Duyne R, Hupp J, Metal–Organic Framework Materials as Chemical Sensors, Chem. Rev 2012;112:1105-1125.

[4] Jeremias F, Fröhlich D, Janiak C, Henninger S, Water and methanol adsorption on MOFs for cycling heat transformation processes, New J. Chem 2014;38:1846-1852.

[5] Henninger S, Habib H, Janiak C, MOFs as Adsorbents for Low Temperature Heating and Cooling Applications, J. Am. Chem. Soc 2009;131:2776–2777.

[6] Henninger S, Schmidt F, Henning H, Water adsorption characteristics of novel materials for heat transformation applications, Applied Thermal Engineering 2010;30:1692-1702.

[7] Rezk A, Al-Dadah R, Mahmoud S, Elsayed A, Experimental investigation of metal organic frameworks characteristics for water adsorption chillers, Proc. IMechE. Part C: J Mechanical Engineering Science 2012;227:992-1005.

[8] Henninger S.K, Schmidt F.P, Henning H.M, Water adsorption characteristics of novel materials for heat transformation applications, Applied Thermal Engineering 2010;30:1692-1702.

[9] Jeremias F, Khutia A, Henninger S.K, Janiak C, MIL-100(Al, Fe) as water adsorbents for heat transformation purposes a promising application, J. Mater. Chem., 2012; 22:10148.

[10] Henninger S.K, Habib H.A, Janiak C, MOFs as Adsorbents for Low Temperature Heating and Cooling Applications, J. AM. CHEM. SOC. 2009;131:2776–2777.

[11] Henninger S.K, Jeremias F, Kummer H, Janiak C, MOFs for Use in Adsorption Heat Pump Processes, Eur. J. Inorg. Chem. 2012:2625–2634.

[12] Henninger S.K, Jeremias F, Kummer H, Schossig P, Henning H.M, Novel sorption materials for solar heating and cooling, Energy Procedia 2012;30:279 – 288.

[13] Ehrenmann J, Henninger S, Janiak C, Water Adsorption Characteristics of MIL-101 for Heat-Transformation Applications of MOFs, Eur. J. Inorg. Chem 2011;4:471–474.

[14] Rui Z, Li Q, Cui Q, Wang H,Chen H and Yao H, Adsorption Refrigeration Performance of Shaped MIL-101-Water Working Pair, Chin. J. Chem. Eng. 2014;22(5): 570-575.

[15] Henninger S, Jeremias F, Kummer H, Janiak C, MOFs for Use in Adsorption Heat Pump Processes, Eur. J. Inorg. Chem 2012;16:2625-2634.

[16] Khutia A, Rammelberg H.U, Schmidt T, Henninger S, Janiak C, Water Sorption Cycle Measurements on Functionalized MIL-101Cr for Heat Transformation Application, Chem. Mater. 2013; 25:790−798.

[17] Janiak C, Henninger S.K, Porous Coordination Polymers as Novel Sorption Materials for Heat Transformation Processes, Chimia 2013;67:419–424.

[18]Yan J, Yu Y, Ma C, Xiao J, Xia Q, Li Y, Li Z, Adsorption isotherms and kinetics of water vapor on novel adsorbents MIL-101(Cr)@GO with super-high capacity, Applied Thermal Engineering 2015;84:118-125.

[19] Elsayed A, AL-Dadah R, Mahmoud S, Shi B, Youessef P, Elshaer A, Kaialy W, Characterisation of CPO-27Ni Metal Organic Framework Material for Water Adsorption, conference paper, SusTEM 2015, Newcastle University, UK.

[20] Jeremias F, Frohlich D, Janiak C, Henninger S, Advancement of sorption-based heat transformation by a metal coating of highly-stable, hydrophilic aluminium fumarate MOF, RSC Adv 2014;4:24073–24082.

[21] Brunauer S, Emmett P, Teller E, Adsorption of Gases in Multimolecular Layers, J. Am. Chem. Soc1938;60:309-319.

[22] Rezk A, Al-Dadah R,Mahmoud S, Elsayed A, Characterisation of metal organic frameworks for adsorption cooling, International Journal of Heat and Mass Transfer 2012;55: 7366–7374.

[23] Canivet J, Fateeva A, Guo Y, Coasne B, Farrusseng D, Water adsorption in MOFs: fundamentals and applications, Chem. Soc. Rev 2014;43:5594—5617.

[24] Furukawa H, Gándara F, Zhang Y, Jiang J, Queen W, Hudson M, Yaghi O, Water Adsorption in Porous Metal-Organic Frameworks and Related Materials, J. Am. Chem. Soc 2014;136:4369-4381.

[25] Uddin K, El-Sharkawy I, Miyazaki T, Saha B, Koyama S, Kil H, Miyawaki J, Yoon S, Adsorption characteristics of ethanol onto functional activated carbons with controlled oxygen content, Applied Thermal Engineering 2014;72:211-218.

[26] Freni A, Sapienza A, Simonova I.A, Glaznev I.S, Aristov Y.I, Restuccia G, Testing of a compact adsorbent bed based on the selective water sorbent 'Silica modified by calcium nitrate' in Heat Powered Cycles. 2009: Techniche Universtat Berlin.

[27] Qiu H, Lv L, Pan B, Zhang Q, Zhang W, Zhang Q, Critical review in adsorption kinetic models, Journal of Zhejiang Univ. Sci. A 2009; 10(5):716-724.

[28] Glueckauf E, Coates J.I, The influence of incomplete equilibrium on the front boundary of chromatograms and the effectiveness of separation. J. Chem. Soc 1947. October, 1315–1321.

[29] Sircar S, Hufton J.R, Why Does the Linear Driving Force Model for Adsorption Kinetics Work? , Adsorption 2000; 6 :137–147.

[30] El-Sharkawy. I. I, Saha B.B, Koyama S, Ng K. C, A study on the kinetics of ethanol-activated carbon fiber: Theory and experiments, International Journal of Heat and Mass Transfer 2006;49:3104–3110.

[31] Rezk A, AL-Dadah R, Mahmoud S, Elsayed A, Investigation of Ethanol/metal organic frameworks for low temperature adsorption cooling applications, Applied Energy 2013;112:1025–1031.

[32] Ulku S, Adsorption heat pumps, Heat Recovery Sys. 1986;6:277-284.

[33] Demir H, Mobedi M, Ulku S, A review on adsorption heat pump: Problems and solutions, Renewable and Sustainable Energy Reviews 2008;12: 2381–2403.

[34] Ng K.C, Thu K, Saha B.B, A novel adsorption desalination method: a test programme for achieving the 1.5 kWh/m3 benchmark, International Water Week, 2008, Singapore.

[35] Ng K.C, Thu K, Kim Y, Chakraborty A, Amy G, Adsorption Desalination: An Emerging Low-Cost Thermal Desalination Method, Desalination 2013;308:161–179.

[36] Tamainot-Telto Z, Metcalf S, Critoph R, Zhong Y, Thorpe R, Carbon–ammonia pairs for adsorption refrigeration applications: ice making, air conditioning and heat pumping, International Journal of Refrigeration 2009;32:1212–1229.

[37] Hamamoto Y, Alam K, Saha B, Koyama S, Akisawa A, Kashiwagi T, Study on adsorption refrigeration cycle utilizing activated carbon fibers. Part 2. Cycle performance evaluation, International Journal of Refrigeration 2006;29:315–327.

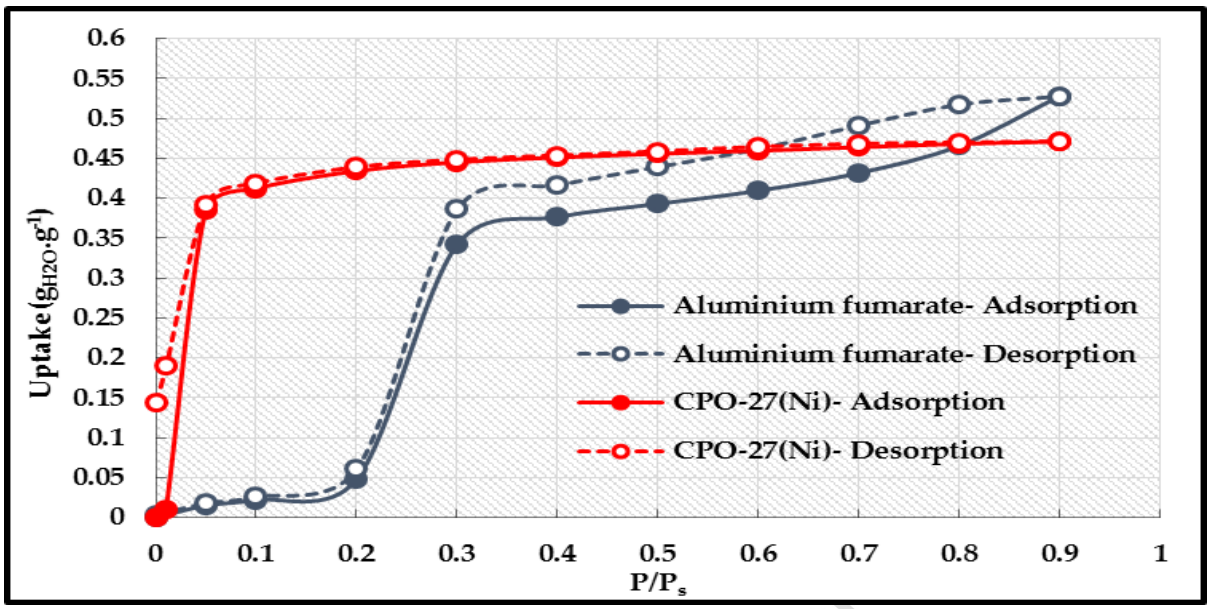

Fig. 1 Water adsorption isotherm of CPO-27(Ni) and aluminium fumarate at 25°C.

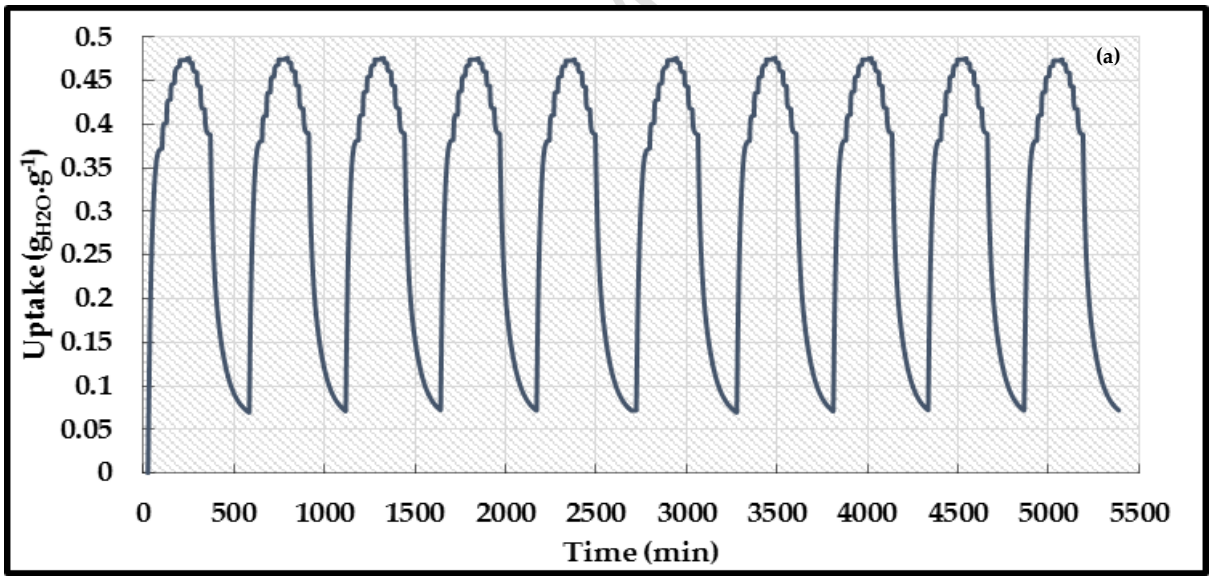

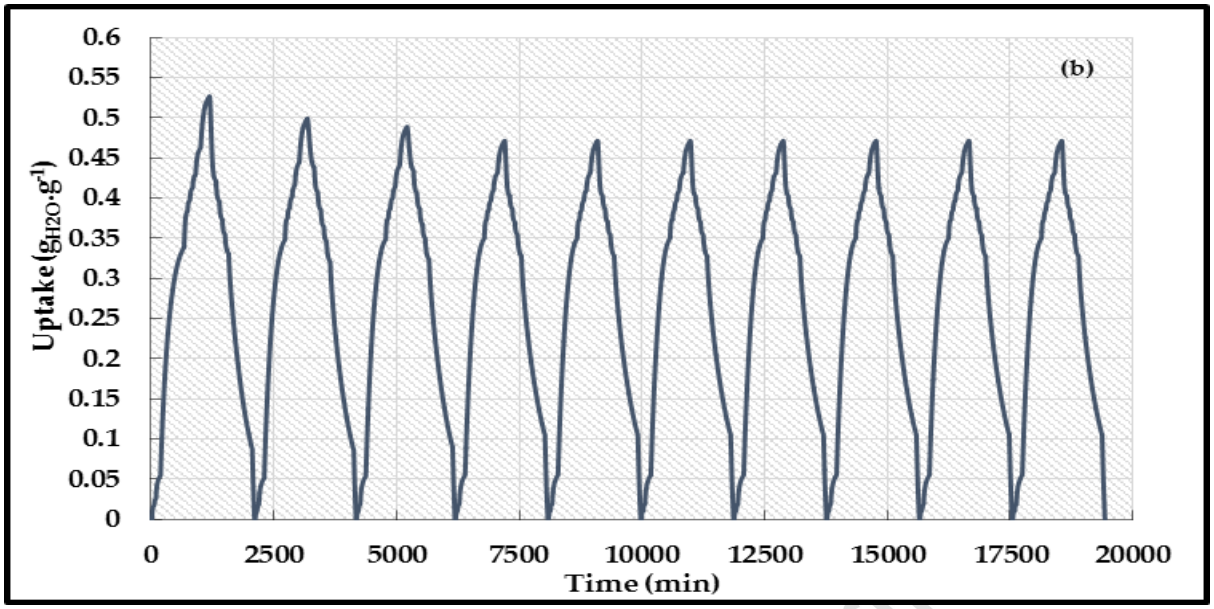

Fig. 2 Adsorption/desorption cycling experiments for a. CPO-27(Ni) and b. Aluminium fumarate.

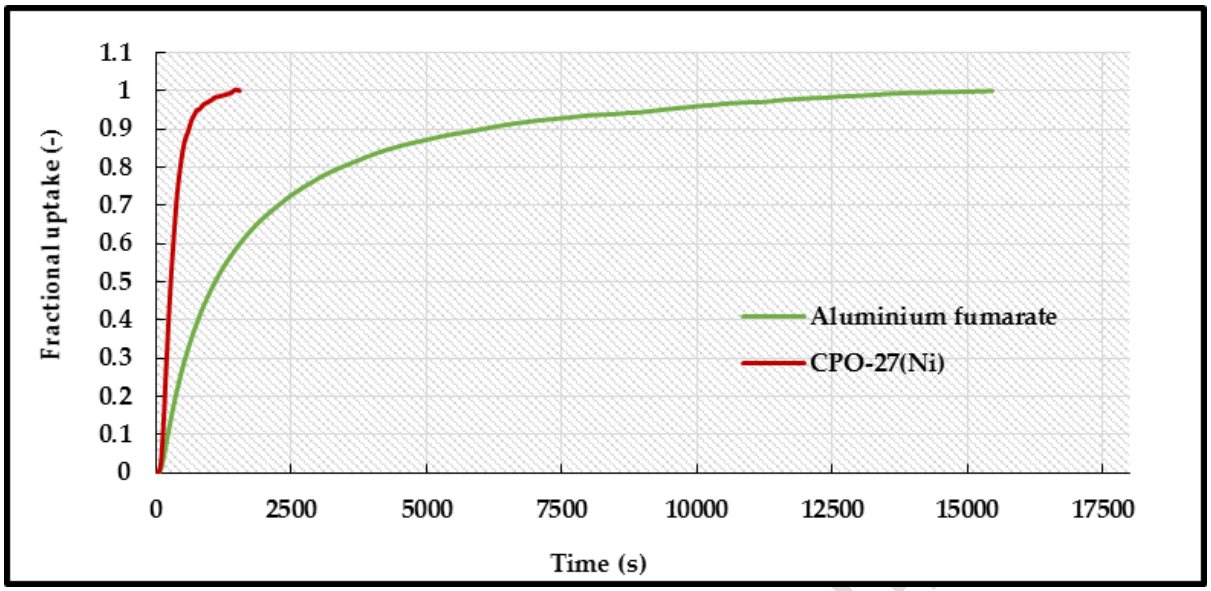

Fig. 3 Fractional uptake of CPO-27(Ni) and aluminium fumarate at 25°C and P/P_s=0.2.

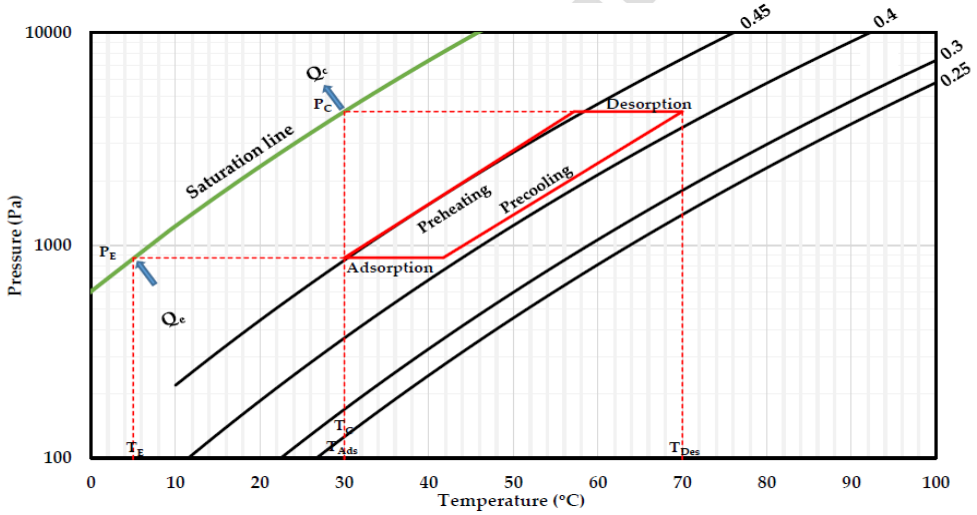

Fig. 4 An example of P-T-x diagram for CPO-27(Ni).
(Ads. Temp. = 30°C, Cond. Temp. = 30°C, Eva. Temp= 5°C and Des. Temp= 70°C)

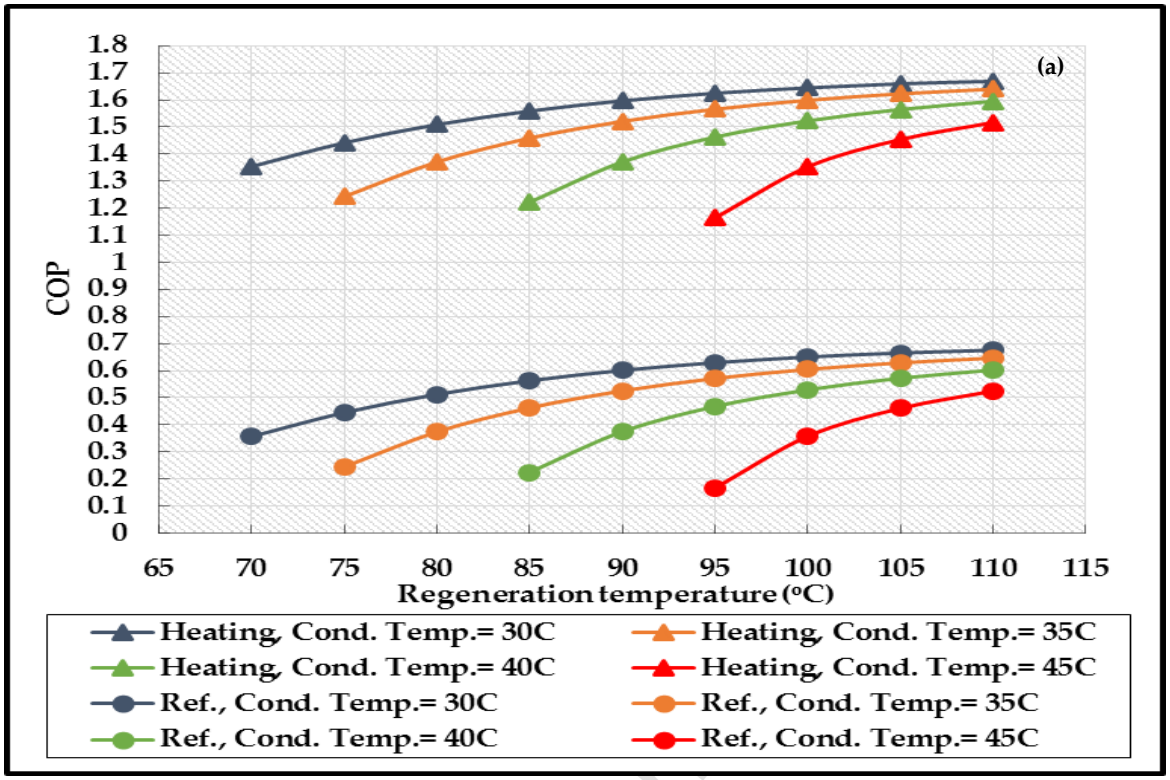

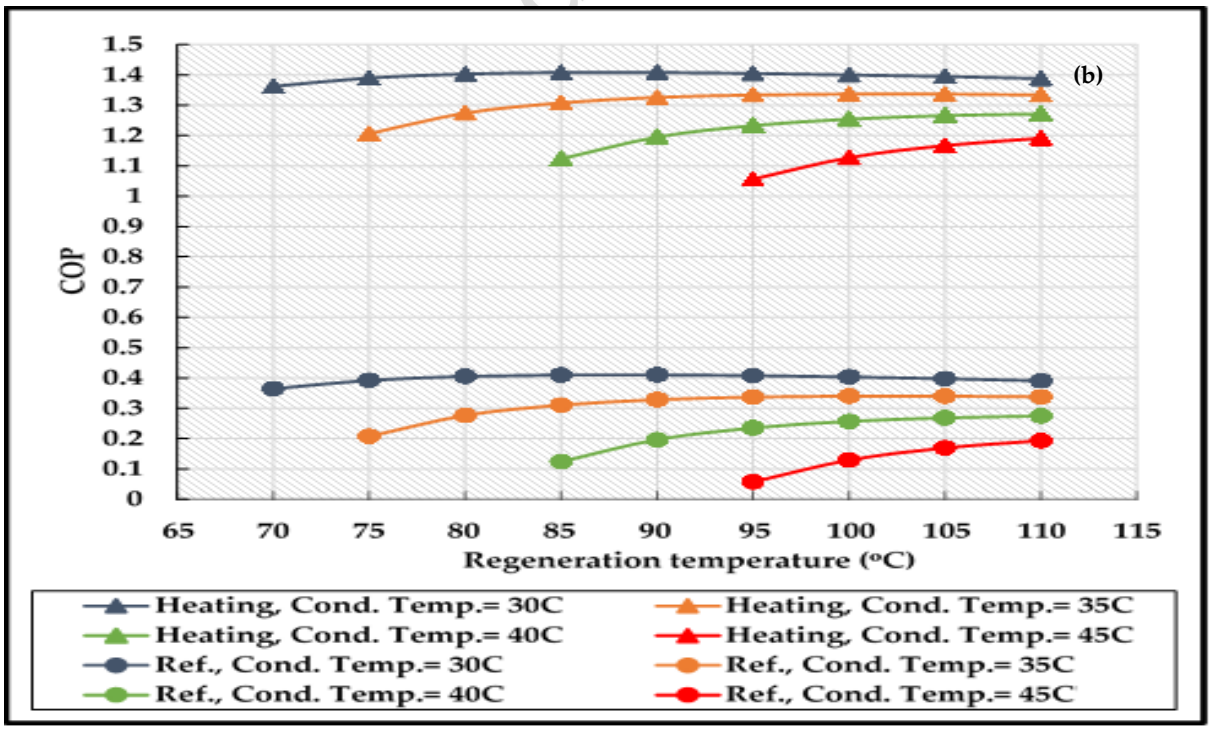

Fig. 5 Effect of condensation and regeneration temperature on the COP_h and COP_{ref} of a. CPO-27(Ni), b. aluminium fumarate cycles at an evaporation temperature of 5°C.

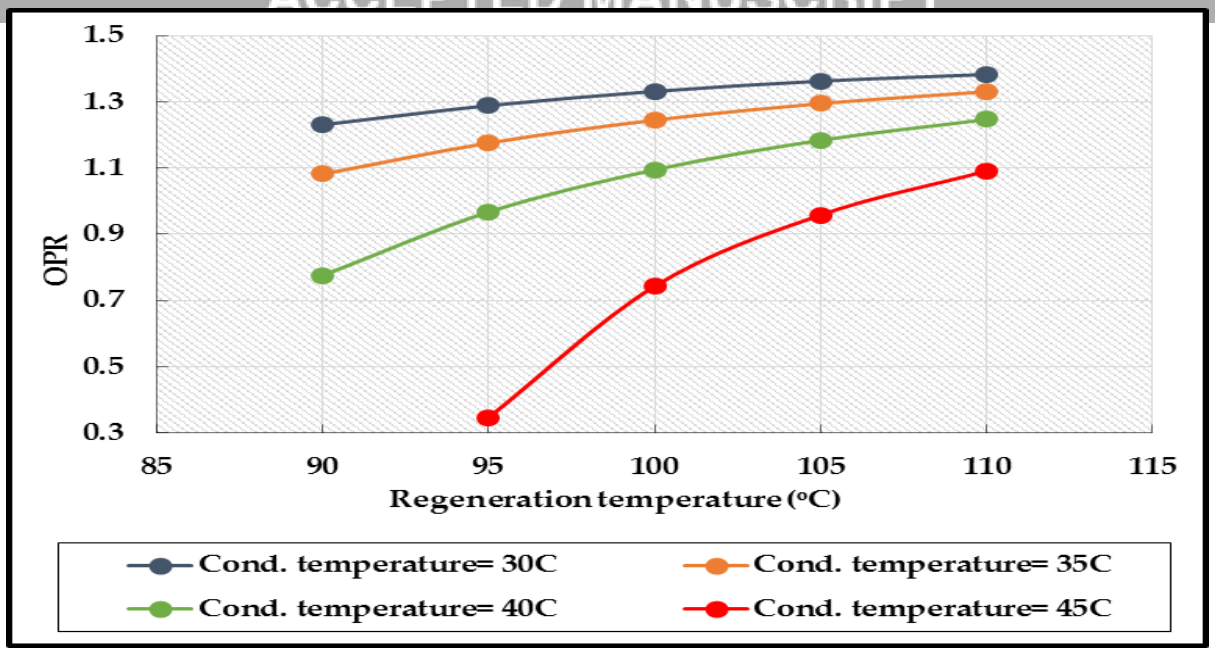

Fig. 7 Effect of condensation and regeneration temperature on the OPR of a desalination cycle using CPO-27(Ni) at an evaporation temperature of 5°C.

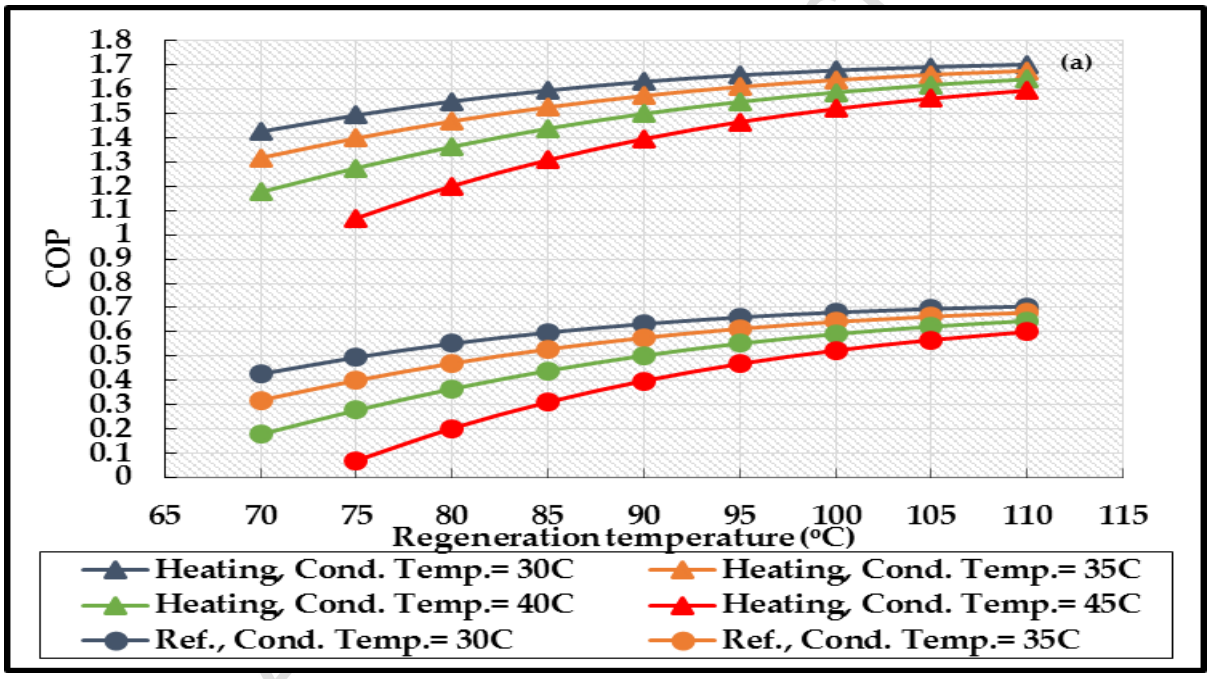

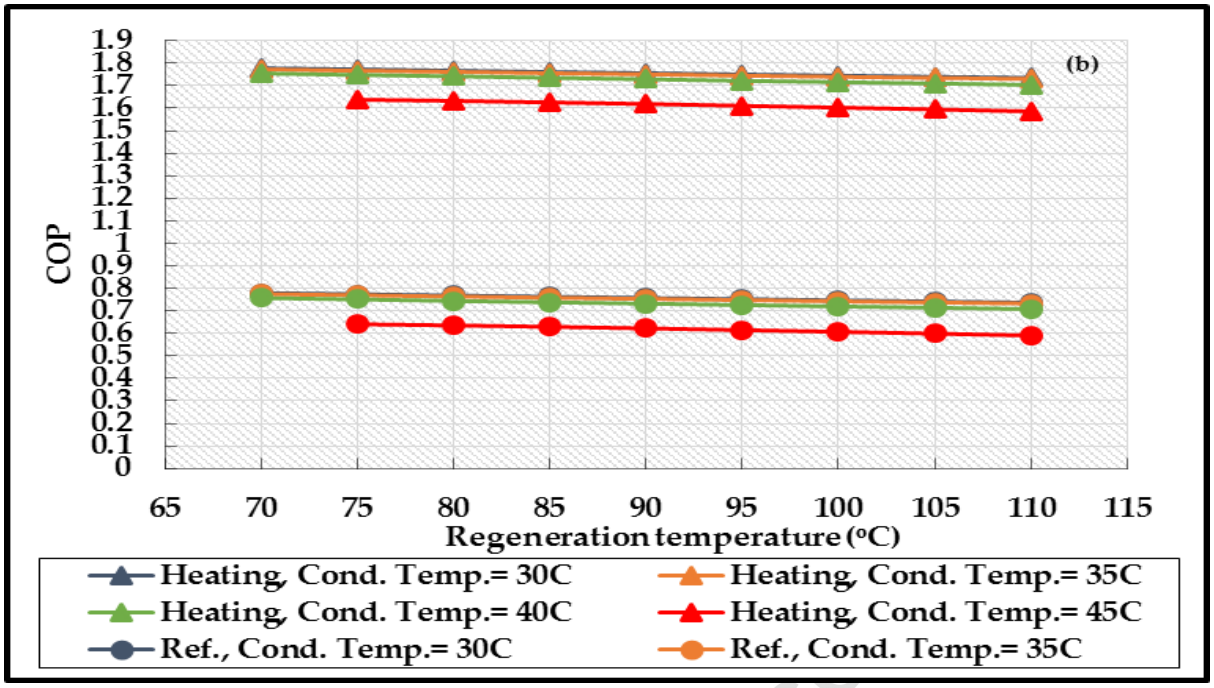

Fig. 8 Effect of condensation and regeneration temperature on the COP_h and COP_{ref} of a. CPO-27(Ni), b. aluminium fumarate cycles at an evaporation temperature of 20°C.

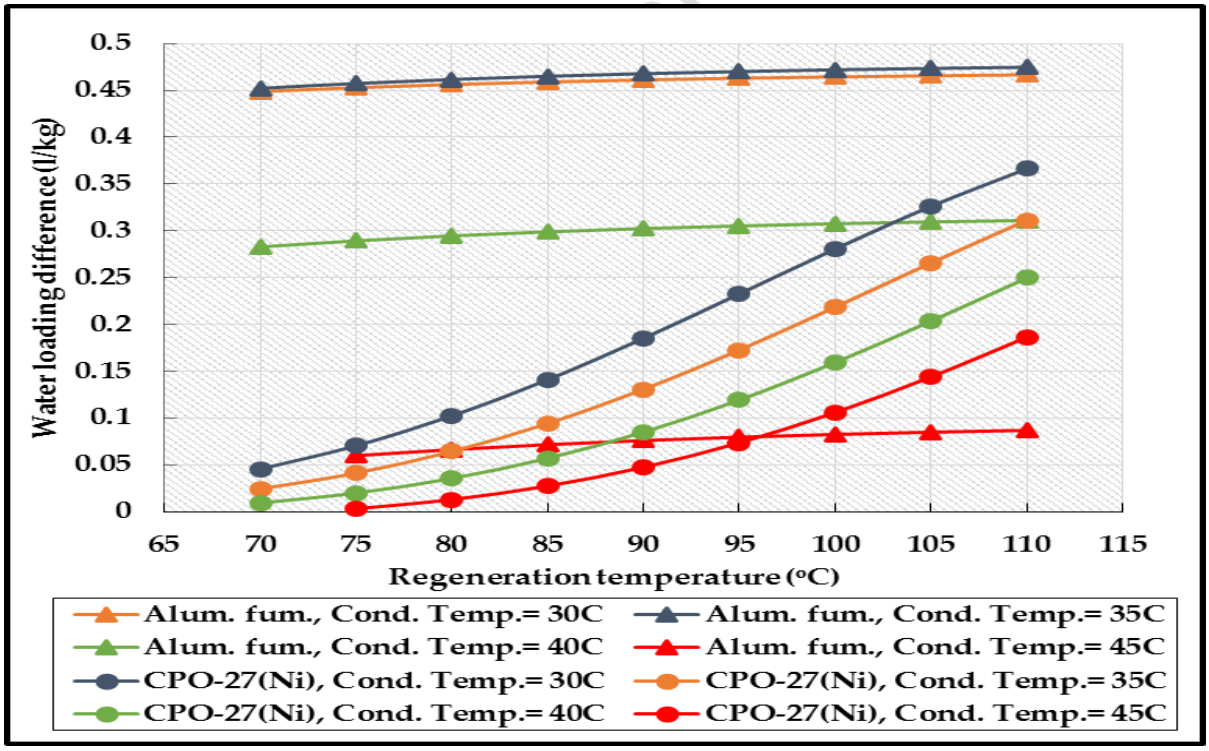

Fig. 9 Effect of condensation and regeneration temperature on the water loading difference in CPO-27(Ni) and aluminium fumarate cycles at an evaporation temperature of 20°C.

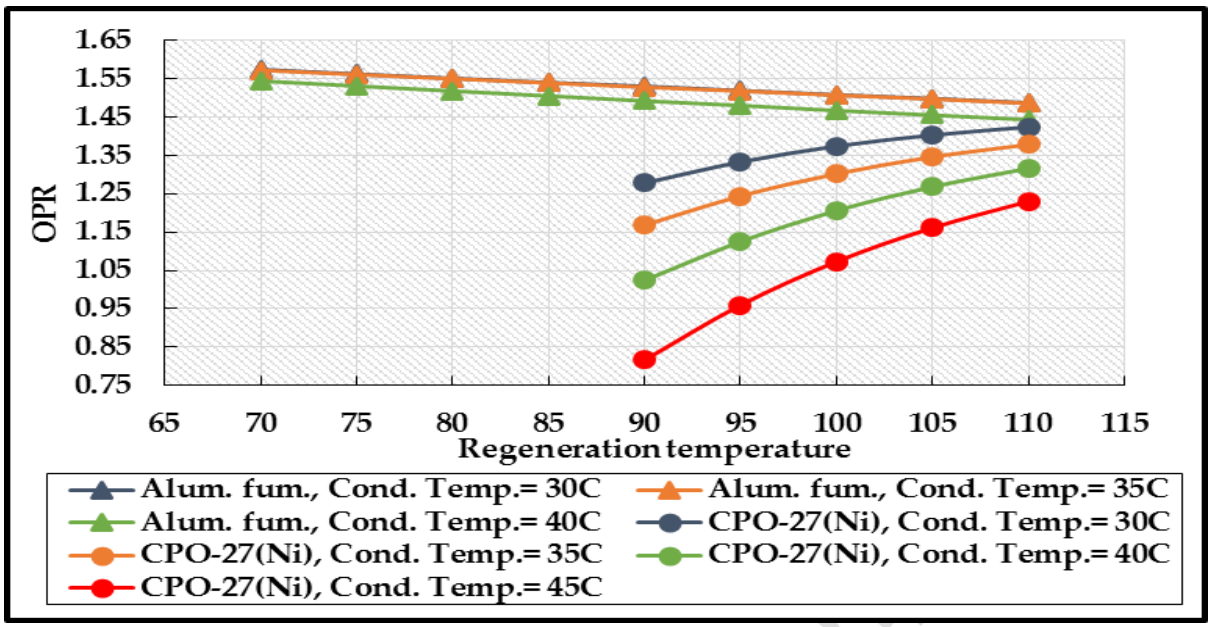

Fig. 10 Effect of condensation and regeneration temperature on the OPR of desalination cycles of CPO-27(Ni) and aluminium fumarate at an evaporation temperature of 20°C.

Table 1 Values of Dubinin-Astakhov equation parameters:

x_0	E	n
0.462	10014.1	4

Table 2 Values of LDF equation parameters:

Adsorbent	E_a	k_0	R_p	$F.D_{so}$
CPO-27(Ni)	25125	5.1	$53.75*10^{-6}$	$1.47*10^{-8}$
Aluminium fumarate	18026	1.29	$0.65*10^{-6}$	$5.49*10^{-13}$

Table 3 Effect of temperature on D_s:

Adsorbent	CPO-27(Ni)		Aluminium fumarate	
T	**298**	**308**	**298**	**308**
$F.D_s$	$5.8*10^{-13}$	$8.1*10^{-13}$	$3.8*10^{-16}$	$4.8*10^{-16}$

Table 4 Summary of the potential applications of aluminium fumarate and CPO-27(Ni) indicating the suitable operating conditions (in the investigated temperature range).

Application	*Comment*	*Regeneration temperature (°C)*	*Condensation temperature (°C)*	*Evaporation temperature (°C)*	*Adsorbent*
Desalination	*With high cooling effect*	≥90	30	5	**CPO-27(Ni)**
	With moderate cooling	70	30	20	**Aluminium fumarate**
Heat pump	*In cold climate*	≥90	30-45	5	**CPO-27(Ni)**
	In moderate climate	70	40-45	20	**Aluminium fumarate**
Refrigeration	*High cooling effect*	≥90	30	5	**CPO-27(Ni)**
	Moderate cooling in hot	70	30	20	**Aluminium fumarate**

	climate				